Int. J. Electrochem. Sci., 12 **(2017)** 4664 – 4676, doi: 10.20964/2017.06.47

International Journal of
ELECTROCHEMICAL
SCIENCE
www.electrochemsci.org

Corrosion Inhibition of Copper by *Capparis spinosa* L. Extract in Strong Acidic Medium: Experimental and Density Functional Theory

Fadel Wedian[1,*], *Mahmoud A. Al-Qudah*[1] *and Ghassab M. Al-Mazaideh*[2]

[1] Department of Chemistry, Faculty of Science, Yarmouk University, P.O. Box 560, Irbid, 22163-Jordan
[2] Department of Chemistry, Faculty of Science, Tafila Technical University, P.O. Box 179, Tafila, 66110-Jordan
[*]E-mail: alwedian@yu.edu.jo

Received: 11 February 2017 / *Accepted:* 29 March 2017 / *Published:* 12 May 2017

Inhibition efficiency of Capparis spinosa (CS) extract on the corrosion of copper metal in 1.0 M nitric acid solution was studied by weight-loss and potentiodynamic measurements. The inhibition efficiency that increases with the rise of the concentrations of CS extract but decreases with the rise of temperature. A maximum inhibition efficiency of 82.7% was achieved by using 440 ppm of inhibitor. The thermodynamic parameters showed that the adsorption of CS extract on copper is physical, spontaneous, and favored at low temperatures. The adsorption of CS extract on the surface of copper obeyed the Langmuir adsorption isotherm at 25, 35 as well as at 45°C. The weight loss, potentiodynamic, and quantum chemical calculations are in a good agreement and reveal that the CS extract is a good inhibitor of copper in acidic solution.

Keywords: Capparis spinosa; copper; corrosion inhibitor; acidic inhibition; DFT.

1. INTRODUCTION

Corrosion is a natural deterioration of the surfaces of metals in atmospheric and aqueous environments. This deterioration causes the metals to alter their properties which are critical for different specific applications [1, 2]. Due to its industrial impact, the inhibition of corrosion processes has been subject of interest. Copper corrosion inhibitors have been widely investigated because of their practical applications, the plants extracts are one of the most important type of inhibitors [3].

The plants extracts inhibitors are used because of the presence of heteroatoms in their structure, their high solubility in water, their high molecular size, their nontoxicity, and their environment friendliness [4-6]. Many plant extracts have been reported as green corrosion inhibitors in various corrosive media such as *Thymus vulgaris* [7] , *Eugenol* from clove [8], *Cryptostegia grandiflora* [9], *Rhizophora mangle* [10], *Mimusops Elengi linn* [11], *Commiphora caudate*[12], fruits of *Emblica officinalis*, *Tinospora cordifolia*, and *Voila odorata* [13]. Most works reporting on their corrosion inhibitions are of experimental nature without any theoretical explanations. Therefore, the quantum chemical techniques are important to explain the absorptive behavior and mechanism of the inhibitory action of the plant extracts.

The *Capparis spinosa* (CS) contains many natural products such as glycosides, tannins, phenolic compound, flavonoids, steroids, carbohydrates, alkaloids and other components. These natural products work as antioxidant, antibacterial, cytotoxic, antidiabetic and have many pharmacological effects [14-16].

This work combines the weight loss method on the one hand and polarization techniques with quantum chemical techniques on the other to investigate for the first time the protection efficiency of the *Capparis spinosa* L extract for copper in nitric acid.

The details of The *Capparis spinosa* L. *Plant material* and *Preparation of the plant extract* were published by wedian et al.[17].

2. EXPERIMENRAL

2.1 Materials and instrumentation

The Copper sheet used was with purity of >99.99% (supplied by Goodfellow USA). The copper sheet was cut to samples (dimensions: 3.0 cm × 1.0 cm × 0.50 mm) and mechanically soldered to a platinum wire; only the rectangular shape foils were exposed to the corrosive environment and it serves as working electrode in the conventional three-electrode electrochemical cell. All used reagents were AR grade chemicals and were purchased from different suppliers. All solutions were prepared from reagents dissolved in triply distilled water. The cyclic voltammetry and polarization measurements were carried out using a Metrohm Autolab potentiostat/galvanostat model PGSTAT 101 connected to a Pentium IV personal computer. The data were analyzed using the Nova 1.6 electrochemical software. The temperature test was adjusted using a TAMSON model T100 thermostat.

2.2 Preparation of copper specimens

Before conducting each experiment, the copper specimens were chemically etched by immersion in 20% HNO_3 for 5 seconds, rinsed with triply distilled water, inserted in the electrochemical cell containing 1.0 M NaOH. The surface was activated by repetitive cyclization of the electrode potential between −1.50 V and 0.745 V until the regular voltammogram of copper electrode

was produced (Figure 1). The voltammogram shows unique features of the copper surface. The four anodic peaks (I, II, III, and IV) are attributed to formation of oxygenated copper surface species Cu_2O, $Cu(OH)_4^{2-}$, CuO, and $Cu(OH)_4^-$, respectively; and their counter cathodic peaks [18].

The CS extract was adsorbed at an open-circuit potential by immersing (dipping) a clean electrode in a solution containing 120, 280, or 440 ppm of CS extract for 2 hours at 25 °C (298 K).

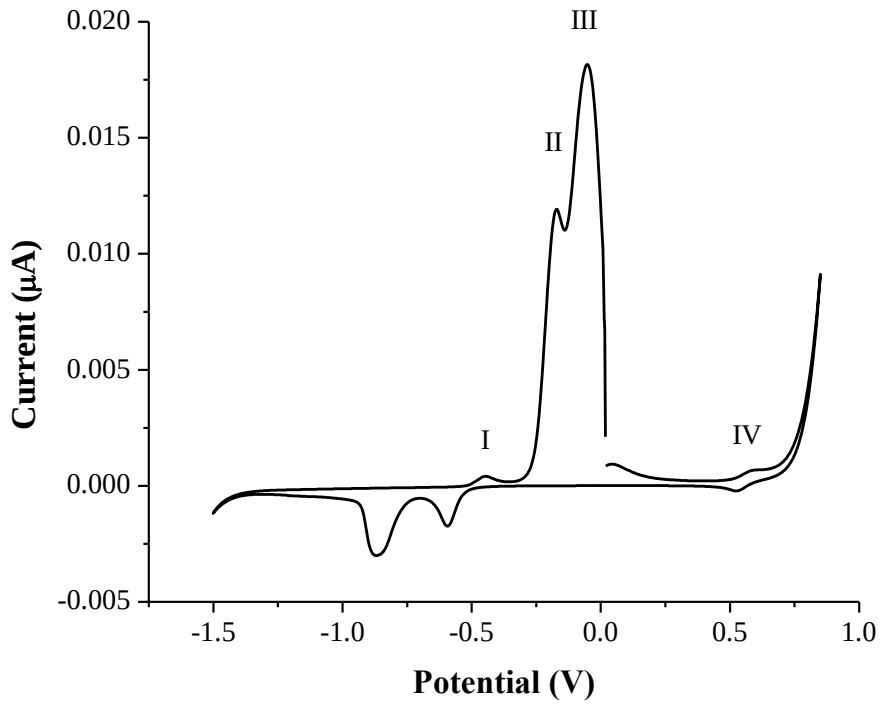

Figure 1. The cyclic voltammetry of copper electrode in 1.0 M NaOH solution at scan rate of 30 mV/s.

2.3 Corrosion tests

2.3.1 Weight loss method

Previously, weighed copper specimens were completely immersed in 1.0 M HNO_3 solutions in the absence (control samples) and the presence of the CS extract. Specimens were rectangular copper foils (dimensions: 3.0 cm × 1.0 cm × 0.50 mm). These experiments were performed at different concentrations of the CS extract: 120, 200, 280, 360 and 440 ppm. All weight-loss measurements were repeated three times and the average of the results was used for comparison. The test period was set to 2 hrs under stirred conditions at 25 °C (298 K) in the acidic medium. Newly fresh solutions were used for each experiment.

The inhibition efficiency (%IE) of the inhibitor, degree of surface coverage (θ), and corrosion rate were calculated by the following expressions:

$$\%IE = [(w_o - w_i)/ w_o] \times 100\% \quad (1)$$

$$\theta = (w_o - w_i)/ w_o \quad (2)$$

$$\text{Corrosion rate (mils per year)} = (3.45 \times 10^6 \times w)/(A \times d \times t) \quad (3)$$

where w_o and w_i are weight losses of copper in grams in the absence and presence of inhibitor; θ is the surface coverage of inhibitor; A in the surface area of the copper specimens (in cm^2) ; d is the density of copper (g/cm^3); t is immersion time (in hours) and W is the weight loss of copper after time t [19].

2.3.2 Electrochemical measurements

The Electrochemical corrosion measurements were carried out in a 1.0 M HNO_3. A conventional three-electrode electrochemical cell was used with the Cu as the working electrode, an Ag/AgCl/[Cl^-]=1.0 M as reference electrode, and a 99.99% pure platinum as auxiliary electrode (Johnson Matthey). The potentiodynamic anodic and cathodic polarizations were obtained by scanning the working electrode starting from E_{corr} (the open-circuit potential) in the range of –250 to +250 mV relative to E_{corr} [20]. The scan rate was set at a 1 mV/sec. The corrosion current (I_{corr}), and the cathodic and anodic Tafel slopes were obtained from the Tafel plot using the Nova 1.6 electrochemical software.

2.4 Computational Details

DFT calculations were performed using hybrid-functions such as B3LYP functional with 6-31G* (d,p) basis set. The DFT-B3LYP was used to optimize the molecules by using Gaussian 03 (G03). The quantum chemical parameters obtained were E_{HOMO}, E_{LUMO}, ΔE_{gap}, chemical potential (η), the global softness (σ), absolute hardness (X) , the fraction of electron transferred (ΔN), and the electrophililcity index (ω).

3. RESULTS AND DISCUSSION

3.1 Tafel Polarization Measurements

Polarization and potentiodynamic corrosion rate measurements of copper were carried out in the 1.0 M of HNO_3 solution in presence of different concentrations of CS inhibitor at 25 °C (Fig. 1). Table 1 below summarizes the results of electrochemical corrosion parameters such as corrosion potential (E_{corr}), corrosion current density (I_{corr}), and the polarization resistance (R_p).

The inhibition efficiency (%IE) is calculated by the following expression:

$$\%IE = \frac{i_{corr} - i_{corr(CG)}}{i_{corr}} \times 100 \qquad (4)$$

where i_{corr} and $i_{corr(CG)}$ are the corrosion current density in $\mu A/cm^2$ without with presence of CG extract. The polarization resistance (R_p) is another parameter which measures the ability of inhibitors to prevent the charge transfer in the test solution and thus retarding the corrosion reaction. The polarization resistance (R_p) in $\Omega\ cm^2$ is calculated by the following expression:

$$R_p = \frac{\beta_a \beta_b}{A \times i_{corr} \times (\beta_a + \beta_b)} \quad (5)$$

where i_{corr} is the corrosion current density in μA/cm^2; β_a and β_b are Tafel slopes of the anodic and cathodic Tafel plots in mV/dec, and A is the surface area of electrode. As can be seen in Table 1, the E_{corr} values shifted to positive potentials with increasing CS extract. Moreover, the polarization resistance increases from 1.7×10^2 Ωcm^2 for pure copper to 6.8×10^2 Ωcm^2 for 440 ppm of inhibitor, providing an increase in the inhibition efficiency to 82.7%. The inhibition efficiencies of other plant extracts were reported. For comparison, the *Mangrove tannin* [21] and *Carboxymethyl cellulose* [22] provided about 80% efficiency on copper. While, the *Nicotinonitriles* [23], *Cryptostegia grandiflora* [9], *Mimusops Elengi linn* [11] offered over 90% inhibition efficiencies on mild steel.

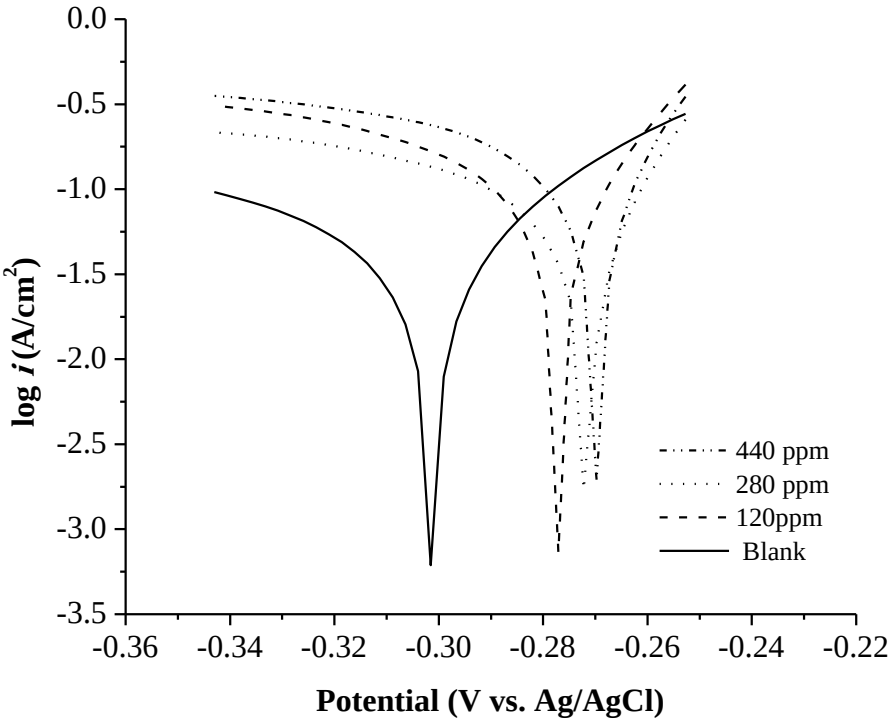

Figure 2. Anodic and cathodic Polarization curves for Cu in 1.0 M HON_3 solution containing blank, 120, 280, 440 ppm of CS extract.

Table 1. Electrochemical corrosion parameters of copper in absence and presence of various concentrations of CS in 1.0 M HNO_3 at 25 °C.

Concentration of CS (ppm)	E_{corr} (mV)	R_p (Ω cm^2)	β_a (mV/dec)	β_c (mV/dec)	I_{corr} (μA/cm^2)	% IE (298 K)
Pure Cu	-305	1.7×10^2	81.4	140.4	202.1	-
120 ppm	-277	3.3×10^2	66.7	118.6	86.2	57.3
280 ppm	-272	5.0×10^2	65.6	94.3	51.9	74.3
440 ppm	-269	6.8×10^2	61.7	84.2	35.0	82.7

β_a anodic Tafel slope of the anodic reaction and β_c cathodic Tafel slope of the cathodic reaction.

3.2 Effect of inhibitor concentration

Table 2. Corrosion parameters obtained from weight-loss method of copper in 1.0 M HNO_3 solution containing different concentrations CS extract at different temperatures.

Temperature (K)	Concentration of CS (ppm)	Corrosion rate (mpy)	Inhibition Efficiency (%)	Corrosion rate ratio*	Surface coverage (θ)
298	pure	585±6.4	-	1.00	-
	120	321±6.7	45.06	0.55	0.4506
	280	134±5.9	79.17	0.23	0.7917
	360	49.1±6.5	91.64	0.08	0.9164
	440	30.3±6.1	94.84	0.05	0.9484
303	pure	636±7.0	-	1.00	-
	120	403±6.5	36.62	0.63	0.3622
	280	197±6.2	69.02	0.31	0.6902
	360	137±5.3	78.41	0.22	0.7841
	440	59.5±6.4	87.65	0.09	0.8765
318	pure	699±6.9	-	1.00	-
	120	470±7.3	32.82	0.67	0.3282
	280	244±6.0	65.05	0.35	0.6505
	360	175±5.2	75.02	0.25	0.7502
	440	89.2±6.2	85.24	0.13	0.8524

* Corrosion ratio = corrosion with present of CS extract/ corrosion rate of plain copper

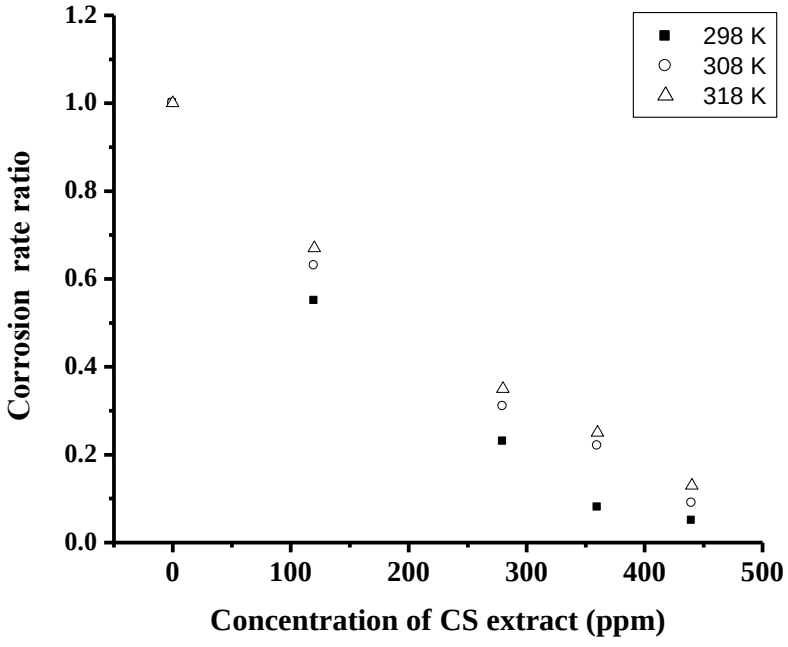

Figure 3. Corrosion rate ratios at different concentrations of CS extract in 1.0 M HNO_3 solution.

The weight-loss method was applied to evaluate the effect of changing the concentrations of the CS extract on the corrosion parameters of copper in 1.0 M HNO_3 at different temperatures as presented in Table 2 below. Table 2 shows that corrosion rate of copper decreased and percentage

inhibition efficiency (IE) increase when increasing the concentration of CS extract at a certain temperature (Figure 3). Moreover, the IE levels decrease when rising temperature, a state of affairs which can be explained by decreasing the strength of adsorption of CS extract on the surface of copper suggesting physical adsorption [24, 25]. A similar behavior was reported for *Rhizophora mangle* [10], *Rotula aquatic plant* [26], *Mangrove tannin* [21], and *Ceratonia siliqua* [27]. However, *Peganum harmala* [28] and *Commiphora caudate* [12] showed a decrease in the inhibition efficiency with the rise of temperature.

3.3 Adsorption Isotherm

The efficiency of CS extract as a corrosion inhibitor depends on many factors such as the nature of copper metal, the interaction between the extract and copper surface, the structure of the organic compounds in the extract and their sizes, and the mode of adsorption. To help understanding the mechanism of corrosion inhibitor and adsorption behavior of CS extract on copper surface, adsorption modes were tested with the most common used adsorption isotherm systems such as: Langmuir, El-Awady, Freundlich, and Temkim. The best fit of the experimental data was considered acceptable when the correlation coefficient was $R^2 \geq 0.98$.

The Langmuir adsorption isotherm is fitted by plotting the concentration of CS extract over the degree of surface coverage (C/θ) vs. the concentration of CS extract (C), according the following equation [29]

$$\frac{C}{\theta} = \frac{1}{K_{ads}} + C \qquad (6)$$

where K_{ads} is the equilibrium constant of the process of adsorption.

Figure 4 shows the plot of (C/θ) and (C). The plot shows strong linear relationship with correlation coefficient of ~0.99. For the Freundlich and Temkim isotherms, the R^2 values were 0.97 and 0.96, respectively. This result suggests that the adsorption of CS extract on copper surface obeyed Langmuir adsorption isotherm. The equilibrium constant K_{ads} of adsorption is related to the standard free energy of adsorption ΔG°_{ads} as expressed by equation 7 and the results are presented in Table 3 below:

$$\Delta G^{\circ}_{ads} = -2.303RTlog(55.5K_{ads}) \qquad (7)$$

where R is the universal gas constant (8.413 $JK^{-1}mol^{-1}$), T is temperature, 55.5 is the concentration of water in solution in mol/L.

Table 3. The adsorption parameters from Lanmguir isotherm for copper specimens in 1.0 M HNO_3 solution at different temperatures.

Isotherm	Temperature (K)	K_{ads}	R^2	ΔG°_{ads} (kJ/mol) ±SD
Langmuir	298	5.165×10^{-3}	0.986	–3.10±0.54
	308	3.793×10^{-3}	0.991	–3.87±0.29
	318	3.224×10^{-3}	0.991	–4.21±0.43

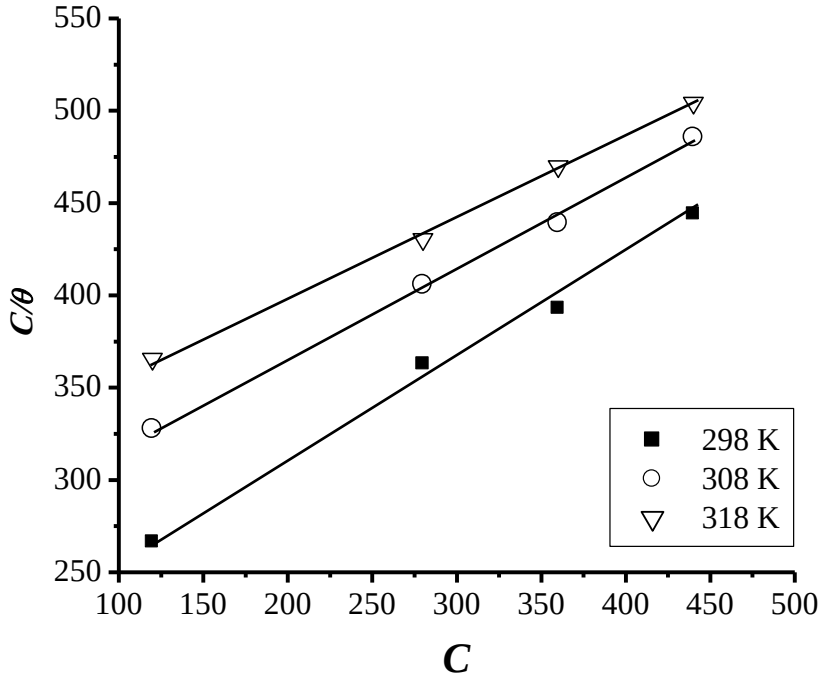

Figure 4. Langmuir adsorption isothermal plot for copper specimens in 1.0 M HNO_3 solution at different temperatures.

The ΔG°_{ads} was found to be –3.10 kJ/mol at 298 K, –3.87 kJ/mol at 308 K, and –4.21 kJ/mol at 318 K. The values ΔG°_{ads} are lower than –40 kJ/mol which suggest electrostatic interaction between the extract and copper surface. Thus, the CS extract adsorption onto copper occurs predominantly by physisorption. The negative sign imply that the adsorption of CS extract on copper surface is spontaneous at standard conditions. Moreover, the decreasing K_{ads} values with temperature could indicate that the adsorption of CS extract on copper surface was more favorable at lower temperatures. Study of adsorption of other plant extracts [10, 12, 22,23,26-28] showed that the adsorption was mainly controlled by a physisorption process. Moreover, the adsorption on metal surfaces obeyed Langmuir adsorption isotherm and they acted mixed type corrosion inhibitors [10, 12, 22,23,26-28].

3.4 Effect of Temperature

The effect of temperature on the mechanism and kinetics on corrosion of copper was evaluated in the absence and on presence of CS extract at 298 K, 308 K, and 318 K using the weight loss measurements in 1 M HNO_3 solution (Table 2). Arrhenius formula equation (8) and transition state equation (9) were used to calculate activation parameters for corrosion process [30]

$$CR = k \exp\left(-\frac{E_a}{RT}\right) \quad (8)$$

$$CR = \frac{RT}{Nh}\exp\left(\frac{\Delta S^{\#}}{R}\right)\exp\left(-\frac{\Delta H^{\#}}{RT}\right) \quad (9)$$

where *CR* is the corrosion rate from weight loss measurements, *k* constant frequency factor, E_a the activation corrosion energy, *R* the universal gas constant, *T* absolute temperature, *h* the Plank`s constant, *N* Avogadro`s number, $\Delta S^{\#}$ the entropy of activation, and $\Delta H^{\#}$ the enthalpy of activation. The

corrosion activation energies (E_a) were calculated for different concentrations of CS extract according to equation 8, and the result is shown in Table 4 below. The results displayed in Table 4 below indicate that the presence of CS extract increases the activation energy of dissolution of copper from 7.005 KJ/mol for blank to 50.79 KJ/mol at 440 ppm of CS extract. Adsorption of extract on the surface of copper may modify the surface by blocking part or the whole of the active sites; thus they may reduce or inhibit the rate of electrochemical reactions on that surface and increase the values of E_a.

The thermodynamic parameters of activation were calculated using equation 9 and presented in Table 4. The positive sign of $\Delta H^{\#}$ reflects the endothermic nature of the corrosion process at the copper surface. The values of $\Delta H^{\#}$ and $\Delta S^{\#}$ indicate the energy barrier of corrosion increases in the presence of extract. The $\Delta S^{\#}$ is a negative higher order in the activated state than in the initial state.

Table 4. The activation parameters from Arrhenius and Transition State Equations for the rate of corrosion of copper in 1.0 M HNO_3 solution containing various concentrations of CS extract.

CS extract concentration (ppm)	E_a (kJ/mol)	R^2	$\Delta H^{\#}$ (kJ/mol)	$\Delta S^{\#}$ (kJ/mol.K)
Blank	7.055	0.992	4.494	−196.1
120	15.07	0.985	17.06	−194.0
280	24.22	0.999	19.00	−194.2
360	42.87	0.997	33.01	−192.7
440	50.79	0.978	40.38	−191.4

3.5 Quantum Chemical Calculation

The Frontier Molecular Orbital theory (FMO) explains the adsorptive ability of molecules over metal surface and its chemical reactivity, which are mainly reflexes to the interaction between HOMO (Highest Occupied Molecular Orbitals) and LUMO (Lowest Unoccupied Molecular Orbitals) levels of the molecules [31].

A theoretical calculations (DFT) were performed only on the major components [14-16] of the Capparis spinosa extract: ß-Sitosteryl glucoside 6'-octadecanoate has molar mass 842.70 g/mol and abbreviated name is SGO, 3-methyl-2-butenyl-ß-glucoside molar mass 248.13 g/mol and abbreviated name is MBG , and the sperimidine – type alkaloid, Cadabicine molar mass 437.23 g/mol and abbreviated name is CAD. The optimized geometry of SGO, MBG, and CAD as well as the nature of their molecular orbitals, HOMO and LUMO, are shown in Figure 5 below.

The energy separation HOMO–LUMO gap (ΔE_{gap}) indicates the reactivity of the molecule towards the adsorption on metallic surface. As the ΔE_{gap} decreases, the reactivity of the molecule increases, and the inhibitor efficiency increases due to increasing the stability of the formed complex between the organic compound and the surface [31]. The concept of softness (σ) and global hardness are also defined on the basis of the ΔE_{gap}. The term global softness is closely related to the polarizability of molecule; a soft molecule has a smaller ΔE_{gap} which leads to easier polarization, and thus it is more reactive [32, 33]. Quantum chemical and molecular dynamics parameters such as energy separation gap (ΔE_{gap}), softness (σ), global hardness (η), chemical potential (X), the fraction of

electron transferred (ΔN), and electrophilicity index (ω) were calculated for CAD, SGO, and MBG (Table 5) .

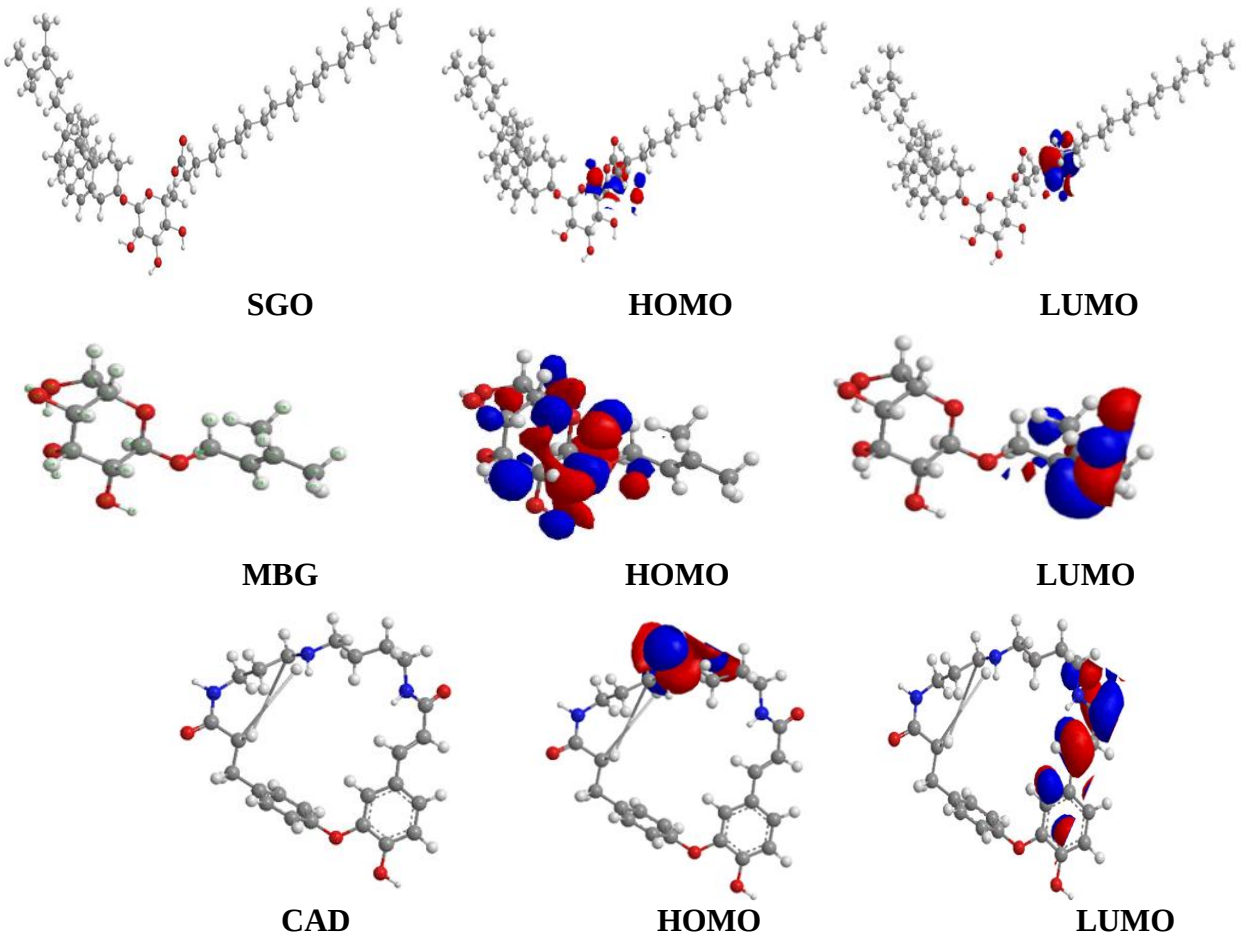

Figure 5. Optimized Structures and Frontier Molecular Orbitals (HOMO and LUMO) of the studied compounds.

Table 5. Quantum descriptions for CS extract major components: CAD, SGO, and MBG using DFT calculations.

Quantum Parameter	CAD	SGO	MBG
E_{HOMO} (eV)	–10.040	–11.062	–11.261
E_{LUMO} (eV)	–4.147	–0.532	–0.677
ΔE_{gap} (eV)	5.893	10.529	11.940
Softness	0.3393	0.1899	0.1889
Global hardness	2.947	5.265	5.293
Chemical potential	7.093	5.797	5.970
electrophilicity index	8.538	3.191	3.367
(ΔN)	0.1208	0.0773	0.0872

Chemical potential of Cu =4.48 eV ; Hardness of Cu =3.25 [27]

The ΔE_{gap} values of the three major components of CS extract increase in the order CAD < SGO < MBG. CAD shows the highest value of softness (σ) and smallest value of global hardness (η). In addition, CAD exhibits the highest electrophililcity index (ω) value as compared to other inhibitors. The electrophililcity index (ω) indicates the ability of the inhibitor to accept electrons from metal surfaces [35]. The E_{LUMO} (−4.147 eV) indicates the high capacity of CAD to accept electrons from Cu. Moreover, the fraction of transferred electrons (ΔN) shows that most electrons transferred to the Cu surface comes from the CAD molecules (ΔN = 0.1208) when compared to other components. The inhibition efficiency of most organic inhibitors increases with increasing electron donating ability at the meal surface when ΔN is less than 3.6 [36].

3.5.1 Mechanism of inhibition

The adsorption of CAD, SGO, and MBG are attributed to the presence of hetero-atoms of nitrogen and oxygen and π-electrons of aromatic rings [37]. The results suggest that CAD, SGO, and MBG can adsorb on the surface by donating the electrons from electron rich centers to the vacant *d* orbitals of copper and also by accepting electrons the Cu surface forming a back-donating bond which depends on the orientation of optimized structure of the inhibitor on the spatial. The results imply that CAD molecule has the strongest ability to adsorb on the copper surface by donating the unshared pair of electrons from N atoms to the vacant *d*-orbitals of copper. Therefore, it is expected that the Capparis spinosa extract inhibition efficiency has mainly resulted from the adsorption of CAD on the surface of copper.

In general, there are two modes of adsorptions of inhibitors on the Cu surface in acidic medium: physisorption and chemisorptions. The magnitude of adsorption depends on the difference between the chemical potential of Cu metal and the inhibitors. The calculated ΔG_{ads} for CAD, SGO, and MBG are –2.613, –1.317, and –1.490, respectively. The ΔG_{ads} values suggest that the mechanism of adsorption of inhibitors is spontaneous physisorption since ΔG_{ads} values are in the range of zero to –40 $kJmol^{-1}$.

4. CONCLUSION

The study of *Capparis spinosa* extract as a potential inhibitor for the copper in 1.0 M HNO_3 was carried out. The results obtained from electrochemical measurements showed that the inhibition efficiency of copper increases with increasing CS extract concentration in acidic solution. The results from the weight loss showed that the inhibition action increases with an increase in inhibitor concentration and decreases with an increase in temperature.

The adsorption of CS extract on the copper surface trails the Langmuir isotherm. The negative values of $\Delta G^{\#}$ indicate that the adsorption of CS extract on copper surface is spontaneous and follows the physical adsorption mechanism. Quantum chemical parameters should provide further insight into the mechanisms of inhibition by the major components of the CS extract.

ACKNOWLEDGEMENTS
The authors would like to thank the Faculty of Graduate Studies and Scientific Research at Yarmouk University for financial support.

References

1. M. G. Fontana, Corrosion Engineering, (Chapter 1 and 2), 3rd ed., McGraw-Hill, Singapore (1986).
2. M. Biezma and R. Cristobal, *Corr. Eng. Sci. Tech.*, 40(4) (2005) 344-353.
3. M. L. Doche, J. J. Rameau, R. Durand and F. Noval-cattin, *Corros. Sci.*,41 (2007) 805-826.
4. I. B. Obot, N. O. Obi-Egbedi and S. A. Umoren, *Corros. Sci.*, 53 (2009) 2738-2747.
5. O. K. Abiola and N. C. Oforka, *Mater. Chemi. Phys.*, 93 (2002) 241-268.
6. N. O. Eddy, S. R. Stoyanov and E. E. Ebenso, *Inter. J. Electrochem. Sci.*, 5 (2010) 1127-1150.
7. A. Ehsani, M. G. Mahjani, M. Hosseini, R. Safari, R. Moshrefi and H. Mohammad Shiri, *J. Colloid. Interface Sci.*, 15 (2017) 444-451.
8. E. Azzouyahar, A. Abu-Obaid, M. El Hajji, L. Bazzi, M. Belkhaouda, A. Lamiri, R. Saighi, S. Jodeh and A. Essahli, *Der Pharma Chemica.* , 8 (2) (2016) 467-475
9. M. Prabakaran, S. Kim, V. Hemapriya and I. Chung, *J. Indust. Engin. Chem.* 37 (2016) 47-56.
10. J. O. Okeniyi, C. A. Loto and A. B. I. Popoola, *J. Appl. Sci.* ,15 (8) (2015) 1083-1092.
11. M. Karuppusamy, P. R. Sivakumar, S. Perumal, A. Elangovan and A. P. Srikanth, *J. Environ. Nanotech.* , 4 (2) (2015) 9-15.
12. S. Aejitha, P. K. Kasthuri and S. Jyothi, *J. Adves. Sci. Tech*., 30 (7) (2016) 784-802.
13. R. Aliyazicioglu, O. E. Eyupoglu, H. Sahin, O. Yildiz and N. Baltas, *Afri. J. Biotechno.*, 12 (47) (2013) 6643-6649.
14. M. A. Khanfer, S. S. Sabri, M. H. Abu Zargaa and K. P. Zeller, *Nat. Prod. Res.*, 17 (2003) 9-14.
15. V. U. Ahmad, A. R. Amber, S. Arif, M. H. M. Chen and J. Clardy, *Phytochemistry*., 24 (1985) 2709-2711.
16. A. Esmail, *Ind. J. Pharm. Sci. Res.*, 5 (2) (2015) 93-100.
17. F. Wedian, M. A. Al-Qudah and A. N. Abu-Baker, *Port. Electrochim. Acta*, 34 (2016) 39-51
18. J. Ambrose, R. Barrdas, and D. Shoesmith, *J. Electroanal. Chem. Interfacial Electrochem.* , 52 (7) (1973) 1194 -1204.
19. 1980 Annual Book of ASTM standards, part 10, G1 – G5, American Society for Testing and Materials, Philadelphia, PA.
20. Basics of Corrosion Measurements, Application Note CORR 1: A publication of EG&G Princeton Applied Research, 1980 and the references therein.
21. A. M. Shah, A. A. Rahim, S. A. Hamid and S. Yahya, *Inter. J. Electrochem. Sci.*, 8 (2) (2013) 2140 - 2153
22. Mei-Ming Li, Qun-Jie Qun, J. Han, H. Yun and Yu-Lin Min, *Inter. J. Electrochem. Sci.*, 10 (11) (2015) 9028-9041
23. P. singh, M. Makowska-Janusik, P. Slovensky and M. A. Quraishi, *J. Mol. Liq.* 220 (2016) 71-81
24. E. A. Noor and A. H. Al-Moubaraki. *Mater. Chem. Phys.*, 110 (2008) 145-154.
25. T. T. Bataineh, M. A. Al-Qudah, E. M. Nawafleh and N. A. F. Al-Rawashdeh, *Inter. J. Electrochem. Sci.*, 9 (2014) 3543-5357.
26. N. S. Patel, J. Hadlicka, P. Beranek, R. Salghi, H. Bouya, H. A. Ismat and B. Belkheir, *Port. Electrochim. Acta*, 32 (6) (2014) 395-403
27. A. S. Fouda, K. Shalabi and A. A. Idress, *Green Chem. Lett. Rev.*, 8 (2015) 17-29
28. K. A. Al-Saadie, H. A. Abas and H. A. Y. Almashhdani, *Mater. Sci. Appl.*, 6 (11) (2015) 1061-1070

29. M. Behpour, S. M. Ghoreishi, M. Khayatkashani and N. Soltani, *Mater. Chem. Phys.,* 131 (2012) 621-633.
30. I. B. Obot, N. O. Obi-Egbedi and S. A. Umoren, *Corros. Sci.,* 51 (2009) 1868-1875.
31. D. F. V. Lewis, C. Loannides and D. V. Parke, *Xenobiotica,* 24 (1994) 401.
32. Z. Zhou and R. G. Parr, *J. Amer. Chem. Soc.,* 112 (1990) 5720.
33. C. U. Ibeji, I. A. Adejoro and B. B. Adeleke, *Phys. Chem. Biophys*., 5 (2015) 1-11.
34. R.G. Pearson , *Inorg. Chem.,* 27 (1988) 734-740.
35. R. G. Pearson, *J. Org. Chem.*, 54 (1989) 1423.
36. J. Fang and J. Li, *J. Molec. Struc.*, 593 (2002) 179.
37. Y. C. Wu, P. Zhang, H. W. Pickening and D. L. AIIara, *J. Electrochem. Soc.,* 140 (1993) 2791-2800.